DETC2015-47871

FORCE TRANSFER CHARACTERIZATION OF A SOFT EXOSUIT FOR GAIT ASSISTANCE

Brendan Quinlivan, Alan Asbeck, Diana Wagner. Tommaso Ranzani,
Sheila Russo, & Conor Walsh
School of Engineering and Applied Sciences, Wyss Institute for Biologically Inspired Engineering, Harvard University, Cambridge, MA, USA

ABSTRACT

Recently, there has been a growing interest in moving away from traditional rigid exoskeletons towards soft exosuits that can provide a variety of advantages including a reduction in both the weight carried by the wearer and the inertia experienced as the wearer flexes and extends their joints. These advantages are achieved by using structured functional textiles in combination with a flexible actuation scheme that enables assistive torques to be applied to the biological joints. Understanding the human-suit interface in these systems is important, as one of the key challenges with this approach is applying force to the human body in a manner that is safe, comfortable, and effective. This paper outlines a methodology for characterizing the structured functional textile of soft exosuits and then uses that methodology to evaluate several factors that lead to different suit-human series stiffnesses and pressure distributions over the body. These factors include the size of the force distribution area and the composition of the structured functional textile. Following the test results, design guidelines are suggested to maximize the safety, comfort, and efficiency of the exosuit.

INTRODUCTION

Over the last several decades, a number of research labs from across the world have developed lower extremity exoskeletons for a variety of applications. Some recent systems apply assistive torques to the lower extremity biological joints (hip, knee, and ankle) to augment the gait of healthy individuals or provide assistance to those with disabilities [1-8]. Additional systems assist with load carriage [9-11] and still others support the physical therapy or rehabilitation of those with disabilities [12-16]. All of these systems are based on a similar principle where a series of rigid links and joints run parallel to an individual's lower limbs and are coupled to the body through a series of interfaces. However, these rigid links often add a significant amount of inertia as the wearer flexes and extends their joints. Although a considerable amount of work has gone

FIGURE 1. OVERVIEW OF THE SOFT EXOSUIT SYSTEM INCLUDING ACTUATOR UNITS, BOWDEN CABLES, STRUCTURED FUNCTIONAL TEXTILE, AND GYROSCOPES.

into minimizing these effects, the rigid structure can still significantly impede an individual's natural gait kinematics.

In recent work we have investigated the use of soft flexible materials to distribute force and apply assistive torques to the biological joints as an alternative to rigid linkages [17-26]. Our group has defined these systems as soft exosuits, and they use structured functional textiles in combination with a flexible actuation scheme to apply assistive torques to the hip and ankle.

One embodiment of the soft exosuit system, shown in Figure 1, performs multi-joint actuation of the hip and ankle joints. It includes actuator packs (shown mounted on an empty backpack), Bowden cables for force transmission, a structured textile for distributing the actuation forces over the wearer, and gyroscopes for gait segmentation [21-22]. The actuator pack anchors one end

of the Bowden cable sheath and controls the position of the inner cable. The opposite end of the Bowden cable sheath and inner cable are fixed to the exosuit on either side of a biological joint such that when the actuation unit retracts the inner cable, these two points are brought together. In conjunction with the exosuit transferring force to the body, this generates a torque about the joint.

To date much of the evaluation of these systems has focused on actuator characterization [17-22] and human performance measures (joint kinematics and metabolic power) [17, 20-22]. Yet one of the key challenges with soft exosuits is to understand how to apply force to the human body in a manner that is safe, comfortable, and effective. While some work has addressed characterizing the suit-human series stiffness and displacement [18-21], an investigation into the pressure at the human-machine interface has yet to occur and a thorough methodology for evaluating the performance of the structured functional textiles has not been developed.

This paper outlines a methodology for characterizing the structured functional textiles of exosuits and then uses that methodology to evaluate several factors that lead to different suit-human series stiffnesses and pressure distributions over the body. Specifically, the study focuses on the differences in the size of the force distribution area and textile composition of the hip extension module of a soft exosuit.

STRUCTURED FUNCTIONAL TEXTILE EXOSUIT

Design Principles

The purpose of the structured functional textile is to transmit force between each end of an actuator and the human body. As described in [21], when designing soft exosuits it is important to (1) maximize the suit-human series stiffness in order to maximize power transfer and (2) maximize comfort to the wearer.

The suit-human series stiffness is the relationship between the force in the suit and the displacement of the actuator [18-23]. The factors that contribute to this stiffness have been found to be the Bowden inner cable stretching and sheath compressing, the suit textile stretching, and the human body compressing under the exosuit [21]. A low stiffness in series with the motor will result in increased power requirements as the motor must move with a higher speed to stretch this series elasticity in addition to moving the joint.

Furthermore, for the system to be worn for extended periods of time it must be comfortable for the wearer. To maximize comfort the suit must minimize normal pressure on the human and minimize shear forces between the suit and human. Normal pressure can be minimized by increasing the contact area between the suit and the human (Pressure=Force/Area) and evenly distributing the force over that area to avoid points of high pressure that may cause discomfort or restrict blood flow [27-28]. By carefully choosing suit force paths and maximizing the suit-human series stiffness, the suit displacements can be lowered and thus lower the shear stress as well [21].
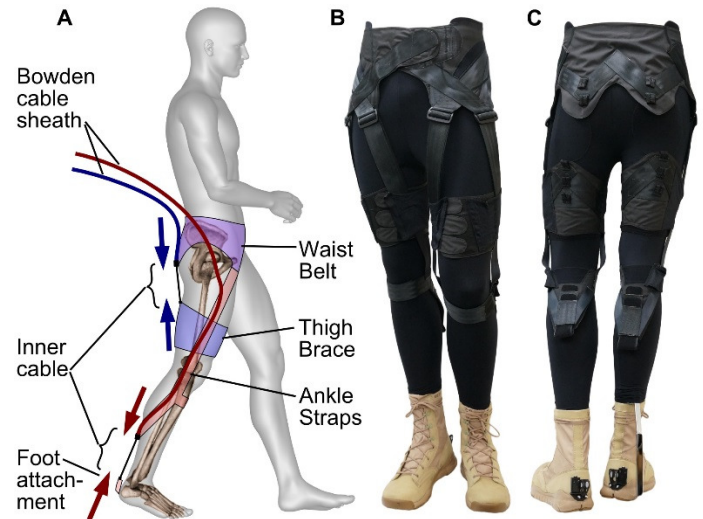

FIGURE 2. (A) DRAWING OF THE SOFT EXOSUIT INCLUDING A MODULE TO ASSIST HIP EXTENSION (BLUE) AND A MULTIARTICULAR MODULE WHICH ASSISTS BOTH PLANTARFLEXION AND HIP FLEXION (RED). (B) FRONT AND (C) BACK VIEWS OF THE STRUCTURED FUNCTIONAL TEXTILE ON A MANNEQUIN.

In summary, maximizing the suit-human series stiffness and comfort is extremely important for exosuits to be used effectively. This is accomplished through specially designed architectures which consist of textiles selected based on their high tensile stiffness and ability to conform well to the human body. These textiles are then oriented with the fabric grain (warp and weft orientation) in the directions of the highest load.

Currently our exosuits contain two modules. One module supports hip extension and the second has a multiarticular design which assists both ankle plantarflexion and hip flexion (Figure 2A). Both modules share the same waist belt and thus can be worn together to provide assistance through both load paths. The hip extension module consists of the waist belt and thigh braces while the multiarticular module consists of the waist belt and ankle straps.

In this paper we focus on the design and evaluation of the hip extension module. To provide a torque about the hip and assist with hip extension, the Bowden cable sheath terminates on the waist belt above the hip joint and the inner cable spans the hip joint attaching to the top of the thigh brace.

Thigh Brace Design and Construction

The thigh braces (Fig. 3) are made primarily of a polyester fabric (WeatherMAX 65, made by Safety Components). They secure around the wearer's leg using tabs of material covered in loop Velcro (Loop 3610, Velcro, Inc.) that connect to a hook Velcro (HTH 845) on the other end of the brace. The thigh braces also include webbing reinforcement (Seatbelt Planet, Inc.) between the point of connection to the Bowden inner cable and the sides of the wearer's leg, since the webbing exhibits much lower strains than an equivalent area of WeatherMAX fabric (Figure 6). This webbing reinforcement is placed into a pattern roughly shaped like an "A". The legs of the "A" are angled to

FIGURE 3. THE FOUR PROTOTYPES OF THE THIGH BRACES EVALUATED IN THIS PAPER INCLUDING (A) LARGE BRACE (B) THE LARGE BRACE WITH ELASTIC, (C) MEDIUM BRACE, AND (D) SMALL BRACE.

follow the approximate force path from the point of connection to the front of the leg. At the apex of the "A", two loops of 1/4"-wide webbing are sewn on to secure the end of the Bowden cable in conjunction with a horizontal Aluminum rod attached to the cable.

The thigh braces are designed to attach tightly and conformably around the wearer's thigh. The human leg is roughly conical, increasing in diameter towards the waist. This geometry means that the thigh brace will not slide upwards as the upward force is applied so long as the textile material is sufficiently inextensible and is appropriately fitted to the wearer. Since the human leg has contours from the shape of the muscles, the tabs on one end of the thigh brace are designed such that the brace can conform to the shape of the leg.

To investigate the effect of exosuit area on the force distribution around the leg, several different thigh braces were constructed. The brace shown in Figure 3A is the tallest with a height of 21.0 cm in the back and 14.0 cm in the front, with an area of 630 cm^2 in contact with the wearer. The brace in Figure 3C is shorter, with a height of 16.5 cm in the back and 9.5 cm in the front, and a contact area of 500 cm^2. Finally, the brace in Figure 3D is composed just of a single 4.6 cm-wide piece of webbing that encircles the thigh and secures with Velcro, with a contact area of 200 cm^2.

The thigh brace in Figure 3B was constructed to be the same dimensions as the brace in 3A, but two short strips of elastic were connected at the base of the top and bottom tabs securing the thigh brace around the thigh. The elastic permitted the thigh brace to conform to the leg geometry more precisely than the other design, but used a more extensible material.

Comparing the designs in Figure 3A and 3B, it was hypothesized that the design with the elastic (3B) would show a more even pressure distribution over the leg since the elastic would permit the top and bottom to be adjusted precisely to the

FIGURE 4. THE TWO PROTOTYPES OF THE WAIST BELT EVALUATED IN THIS PAPER INCLUDING (A) WEBBING-REINFORCED WAIST BELT AND (B) WEATHERMAX-REINFORCED WAIST BELT.

wearer's leg. In early testing it was observed that frequently with the design in Figure 3A there was a small gap between the bottom of the thigh brace and the wearer's leg. This was due to the adjustment tabs not being adequately able to cause the textile to match the wearer's thigh shape. However, due to the added elastic, it was also hypothesized that the brace in Figure 3B would have slightly lower suit-human series stiffness than that of the brace in Figure 3A.

Comparing the designs in Figures 3A, 3C, and 3D, it was hypothesized that the stiffness will increase with increasing area as distributing the force over a wider area will improve the suit-human series stiffness. Additionally, lower pressure concentrations were expected for the braces with larger areas.

Waist Belt Design and Construction

The two waist belts tested are shown in Figure 4. Their designs are similar, but with differences in their reinforcement. The design in Figure 4A consists of a layer of WeatherMAX fabric and a layer of a lightweight nylon liner material (DWR Supplex, Inc.), both of which extend over the entire waist belt area. This nylon liner is much more compliant than the WeatherMAX and serves primarily to simplify the waist belt's construction. Velcro hook and loop patches are added to secure the waist belt in the front of the wearer's waist. Neoprene (Seattle Fabrics, 3 mm thick) is added in two large patches to pad the wearer's pelvis bone, since much of the force is transferred to this location during operation. Two large holes are cut in the WeatherMAX and liner materials over the iliac crest of the pelvis, so in this location only neoprene exists to transfer force to the wearer. These holes enable the fabric to conform to the pelvis bone more closely and distribute the pressure more evenly over the waist. Finally, webbing reinforcement is placed in a series of "V"-shapes along the approximate force paths at the bottom of the suit. 1/4" webbing loops are used to attach each Bowden cable sheath to the exosuit in conjunction with a horizontal aluminum bar that is supported by a loop on each side.

The waist belt in Figure 4B has a base layer of a single layer of WeatherMAX fabric, but it does not have a second layer acting as a liner. Also, instead of webbing reinforcement, it has a second layer of WeatherMAX fabric that is positioned in approximately the same location as the webbing in the other waist belt. In all other respects the two waist belts are identical.

These two construction methods were used to investigate the difference between the webbing and the WeatherMAX reinforcements. Webbing is much less extensible than WeatherMAX fabric, but is also much less flexible and thus less able to conform to the human body. Since distributing the force over a wider area will improve the suit-human series stiffness, it is hypothesized that the two waist belts will have similar stiffnesses as the WeatherMAX waist belt (Figure 4B) is more conformal but contains a more extensible fabric than the webbing waist belt (Figure 4A). Additionally, since the WeatherMAX waist belt is expected to be more conformal and distribute the force over a wider area, it is expected to have a more even pressure distribution.

EXOSUIT CHARACTERIZATION METHODOLOGY

Overview

We characterize the ability of these exosuit components to withstand high forces during loading with minimum displacement by evaluating the suit-human series stiffness and the individual contributions of the textile and human to that quantity. We also measure the pressure at the suit-human interface as a measure of the suit's comfort.

Suit-Human Series Stiffness Evaluation

As previously mentioned, power is lost during suit loading as a result of the Bowden cable stretching and sheath compressing, the suit textile stretching, and the human tissue under the suit compressing [21]. To be able to improve the exosuit designs, it is important to understand how much each of these components contributes to the overall suit-human series stiffness. We developed a methodology to systematically analyze each element of the system. Specifically, we determine the compliance of 1) the raw textiles, to understand the material properties per unit area; 2) the Bowden cable transmission; 3) the structured functional textiles, i.e. the completed suit components, the compliance of which includes not only the textiles themselves but also the effects of how they are layered and patterned to fit on the body; and 4) the human tissue. To determine the contributions of each of these to suit-human series stiffness, we conducted the tests shown in Figure 5.

First, the raw textiles used in the components (webbing and WeatherMAX) were characterized by performing a tensile test using an Instron 5566 Universal Testing Machine, as shown in Figure 5A. Strips of fabric 5cm wide by 15cm long were stretched to 200N or 300N four times sequentially. The resulting textile strain vs. force in the fabric are shown in Figure 6. The figure shows the third and fourth trials for each fabric, in order to eliminate the effects of plastic deformation of the textiles. This deformation occurs on the first stretch as the textile fibers realign to accommodate the force.
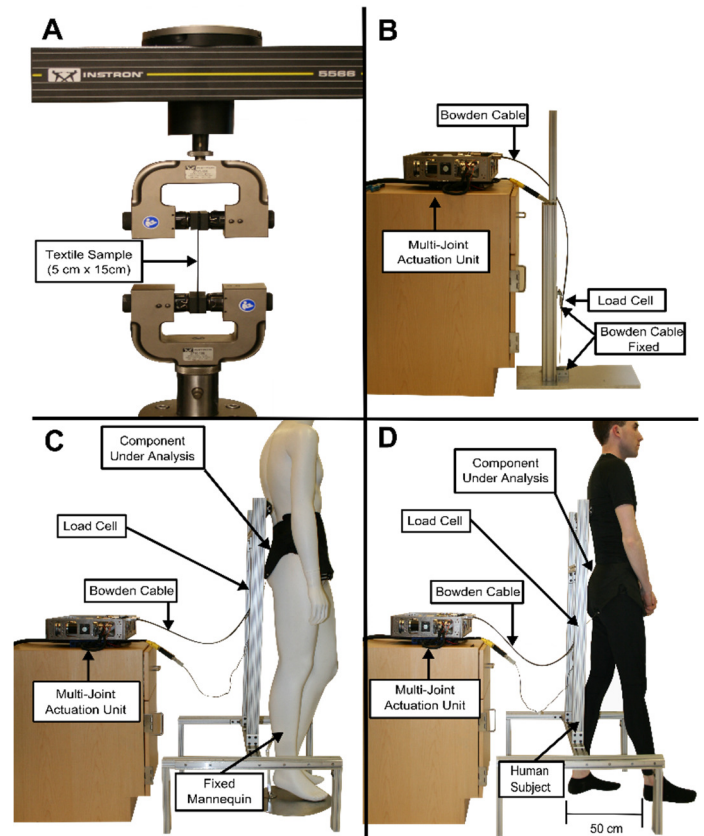

FIGURE 5. TESTING CONDITIONS USED TO ANALYZE THE STIFFNESS OF THE EXOSUIT COMPONENTS: (A) RAW TEXTILE, (B) BOWDEN CABLE, (C) EXOSUIT ON MANNEQUINM, AND (D) EXOSUIT ON HUMAN.
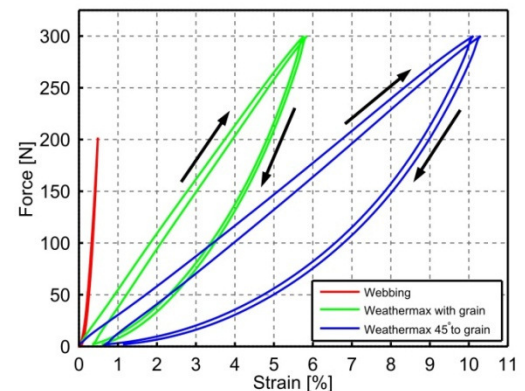

FIGURE 6. STRAINS IN THE TEXTILES VS. APPLIED FORCE. ARROWS INDICATE THE DIRECTION OF THE HYSTERESIS LOOPS.

For the subsequent three tests (Figure 5B-D), the multi-joint actuation unit was used to create forces in the suit via a Bowden cable [20]. The system, previously described in [20], is equipped with several sensors logging data at 1 kHz to track the displacement of the actuator and the force applied to the suit. The Bowden cable actuator contains a linear potentiometer (P3 America, Inc.) with a resolution of 0.1 mm to measure

displacement of the actuation cable. A Futek load cell with a measuring range of ±445 N (2N resolution) is placed at the distal end of the Bowden cable to measure the force applied. All subsequent tests used these measurements of the cable displacement at the actuator and the force at the distal load cell.

To assess the stiffness of the cable and actuation system itself, both ends of the Bowden cable were fixed and a force of 300 N was applied and removed linearly over a period of 3 seconds, as shown in Figure 5B.

The stiffness of each structured functional textile component was characterized by placing the suit component on a mannequin, as shown in Figure 5C. Using a rigid mannequin permits the stiffness of the finished suit component to be measured without including the compliance of the human underneath. The component was placed on the vertical leg (mid-stance of gait cycle) of a fixed fiberglass mannequin. The distal end of the Bowden cable sheath was fixed on a rigid testing frame, and the inner cable was anchored to the component (right side). A maximum force of 250 N was applied and removed linearly over a period of 3 seconds. This process was repeated three times for each component, donning and doffing the component each time.

Finally, the overall suit-human series stiffness was determined by placing the suit component on one human subject and following the same procedure used in the mannequin testing, as shown in Figure 5D. Subjects gave informed consent and testing was approved by the Harvard Institutional Review Board (IRB). As this investigation focused on characterizing the hip extension module, the subject stood with their feet 50 cm apart in a pose close to that of 0% of the gait cycle, which is when force is maximally applied to assist with hip extension as described in [23, 26]. During all tests the subject was asked to contract their muscles as force was applied. Each component was tested across three trials, donning and doffing the component each time.

Pressure Distribution Evaluation

To evaluate the pressure at the suit-human (and suit-mannequin) interface, one high dynamic analog pressure sensor (Texe Srl, Florence, Italy) with a 26x52 cm detective surface, resolution of 2 cm, and detectable range of 1.8-100 kPa was placed between the suit and wearer. The sensor consists of three layers, as seen in Figure 7. The inner layer is made of piezo-resistive material and the two outer layers consists of conductive strips (17 mm width spaced 3 mm apart) which form a matrix of 17 mm^2 cells. As pressure is applied, the piezo-resistive material changes its electrical resistivity and the matrix of conductive strips records this change. Sensor calibration was conducted as described in [30].

A similar procedure to the series stiffness evaluation on the mannequin and human (Figure 5C and 5D) was followed using the multi-joint actuation platform. A force of 250 ± 5 N was applied to the wearer and held for 10 seconds during which time the pressure was recorded at 50 Hz through an Arduino Due (Arduino, ITALY) and synced with the multi-joint
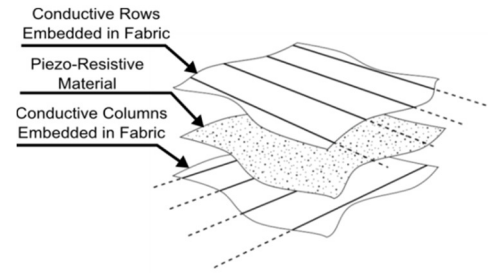

FIGURE 7. HIGH DYNAMIC ANALOG PRESSURE SENSOR. THE THREE LAYERS OF THE SENSOR ALLOW FOR PRESSURE EVALUATION DUE TO THE MATRIX FORMED BY THE ROWS AND COLUMNS OF CONDUCTIVE MATERIAL EMBEDDED IN FABRIC AND SEPARATED BY A PIEZO-RESISTIVE MATERIAL [29-30].
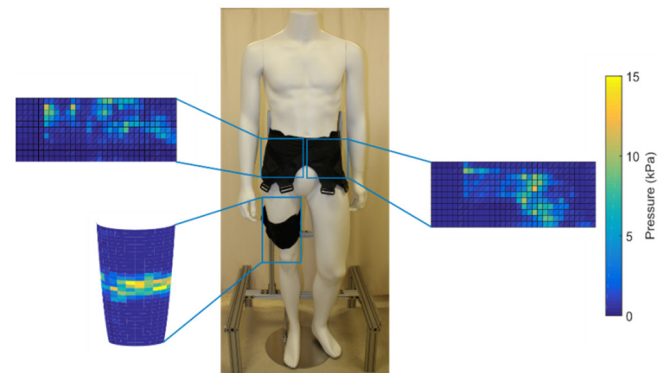

FIGURE 8. EXAMPLE PRESSURE MAP OF THE WAIST BELT (LEFT AND RIGHT) AND THIGH BRACE.

platform. These trials were preformed separately from the stiffness trials so that a reliable pressure measurement could be taken and averaged over 10 seconds of constant pressure. The procedure was conducted on both the mannequin and a human subject and the tests were each repeated three times, donning and doffing the component between trials. Two separate tests were conducted on the waist belt to measure the pressure on both the actuated (right) and non-actuated (left) sides of the pelvis. An example pressure map under the thigh brace and waist belt is shown in Figure 8.

THIGH BRACE CHARACTERIZATION

The four thigh braces designs, shown in Figure 3, were evaluated using the exosuit characterization methodology outlined above. One representative curve for each condition of the series stiffness evaluation is shown in Figure 9. It is important to note for both the Bowden Cable and mannequin tests that after reaching the peak displacement, the force remains constant as the actuator decreases its position by a few millimeters. This phenomenon is believed to result from the Bowden Cable contracting from its stretched length to its natural length, beginning at the actuator side, while friction between the inner cable and outer sheath along the length of the cable prevents relative motion between the two at the end of the cable. This is not observed in the human testing most likely due to the added compliance of the human tissue.
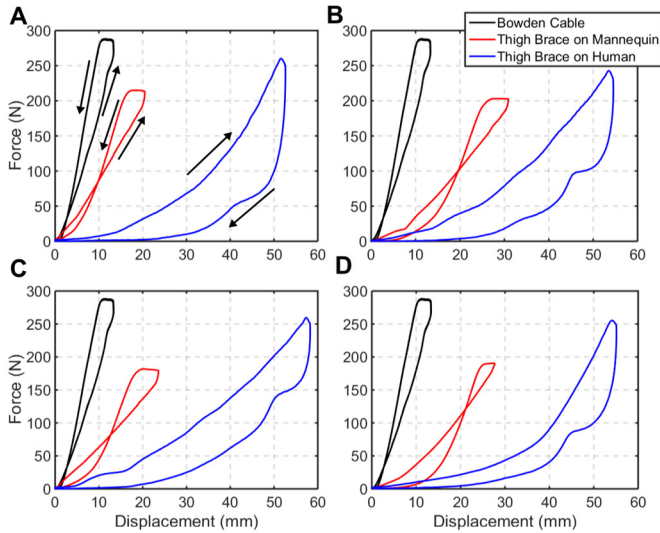
FIGURE 9. THE RESULTS OF THE SERIES STIFFNESS EVALUATION FOR THE FOUR THIGH BRACES (A) LARGE, (B) LARGE WITH ELASTIC, (C) MEDIUM, AND (D) SMALL INCLUDING THE STIFFNESS OF THE BOWDEN CABLE, THIGH BRACE ON A MANNEQUIN, AND THIGH BRACE ON A HUMAN. ARROWS INDICATE THE DIRECTION OF THE HYSTERESIS LOOPS.

From these results it is clear that on the mannequin, the large thigh brace had the highest stiffness (Figure 9A) which decreases when elastic is added (Figure 9B) and as the size of the brace is reduced (Figures 9C and 9D). When on the human, the stiffness of the thigh braces do not appear to differ as considerably but the large thigh brace (Figure 9A) does still appear to have a higher stiffness than those with elastic or reduced size (Figures 9B-D)

Additionally, a pressure distribution evaluation was conducted on all four thigh braces, with the pressure sensors placed on the anterior of the thigh. For each trial, the results over a 10 second trial were averaged for each of the 384 cells in the pressure sensitive matricial fabric. The results were then distributed into bins and the results (average ± standard deviation) for each bin are shown in the histogram in Figure 10, disregarding sensor readings below 2.5 kPa. Prior to the application of force, the pressure across the brace was approximately 4.27 kPa for each trial which is comparable to the pressure of compressive garments (~2.7-6.7 kPa). However, as shown in Figure 10, the peak pressures under 250 N of applied force can reach up to 20 kPa. As this pressure is only applied periodically it is not of significant concern.

Comparing the large brace (Figure 9A) to the large brace with elastic (Figure 9B), the added elastic appears to slightly reduce the pressure experienced by the wearer (by 5-10 kPa). Additionally, as expected there is a noticeable difference between the pressure distributions of the large, medium, and small thigh braces. The medium thigh brace does not appear to distribute the force as well as the large brace on both the human and mannequin. The small thigh brace appears to distribute the force worse than the large and medium braces which results in higher peak pressures.
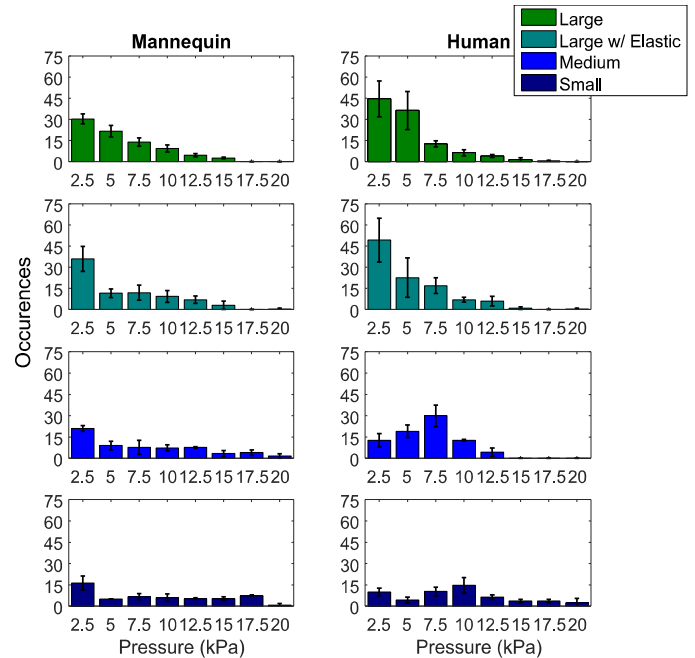

FIGURE 10. A HISTOGRAM OF THE PRESSURE DISTRIBUTION ACROSS THREE TRIALS (AVERAGE ± SD) ON THE ANTERIOR OF THE THIGH FOR THE FOUR DIFFERENT THIGH BRACE DESIGNS ON A MANNEQUIN AND ON A HUMAN WITH AN APPLIED FORCE OF 250 N AVERAGE OVER 10 SECONDS FOR EACH TRIAL.

WAIST BELT CHARACTERIZATION

The two waist belt designs, shown in Figure 4, were also evaluated. Representative curves from the series stiffness evaluation are shown in Figure 11 which clearly indicate that on the mannequin, the webbing reinforced waist belt has a higher stiffness, while the WeatherMAX reinforced waist belt has approximately the same stiffness on the mannequin and human. On the human, both waist belts appear to have approximately the same stiffness.
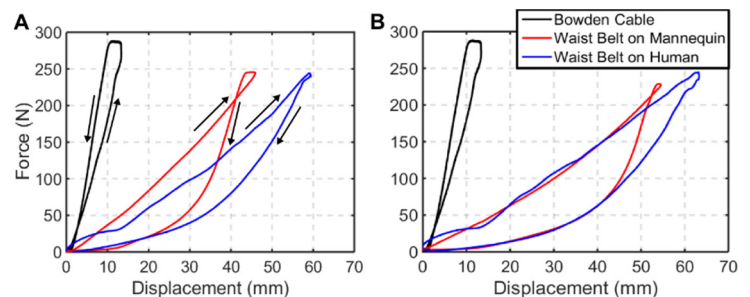

FIGURE 11. THE RESULTS OF THE SERIES STIFFNESS EVALUATION FOR BOTH (A) WEBBING WAIST BELT AND (B) WEATHERMAX WAIST BELT INCLUDING THE STIFFNESS OF THE BOWDEN CABLE, WAIST BELT ON A MANNEQUIN, AND WAIST BELT ON A HUMAN. ARROWS INDICATE THE DIRECTION OF THE HYSTERESIS LOOPS.
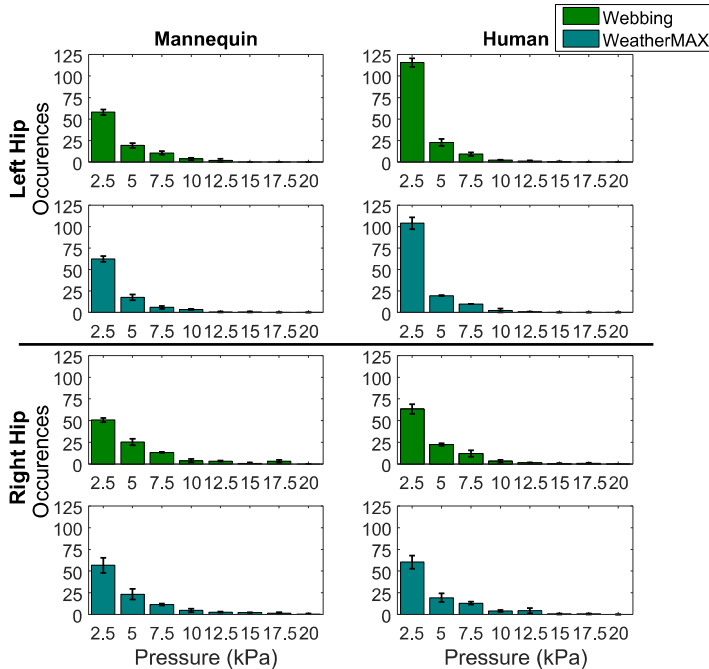
FIGURE 12. A HISTOGRAM OF THE PRESSURE DISTRIBUTION ACROSS THREE TRIALS (AVERAGE ± SD) OF THE TWO WAIST BELT DESIGNS ON THE LEFT AND RIGHT SIDE OF A MANNEQUIN AND A HUMAN WITH AN FORCE OF 250 N APPLIED TO THE RIGHT SIDE OF WEARER AND AVERAGE OVER 10 SECONDS FOR EACH TRIAL.

Finally, the pressure distributions of the waist belts on the left and right sides of the wearer were also evaluated (Figure 12). There appears to be a higher pressure concentration on the actuated side of the wearer (right). It also appears that the webbing waist belt has slightly higher pressure concentrations than the WeatherMAX waist belt, a difference that is more pronounced on the right side of the wearer. Thus, the two belts behave as expected where the stiffer webbing (Figure 6) results in a stiffer waist belt but the more conformal WeatherMAX better distributes the force across the pelvis.

CONCLUSIONS & FUTURE WORK

This paper outlines a methodology for characterizing the structured functional textile in exosuits and then uses that methodology to evaluate several factors that lead to different human-suit series stiffnesses and pressure distributions over the body. The study focuses on the differences in the size of the force distribution area and textile composition of the hip extension module of a soft exosuit.

Structural and size changes of the waist belt and thigh braces resulted in differences in the stiffness of the structured functional textile on the mannequin but those changes were not as pronounced on a human. Based on this, it appears that significant changes in the stiffness of the structured functional textile result in smaller changes in suit-human series stiffness as the human tissue is the predominate factor. However, more rigorous studies must be conducted to investigate how design changes result in slight differences in suit-human series stiffness which could still

significantly improve power and travel requirements from actuator units.

Additionally, structural and size changes of the waist belt and thigh braces resulted in noticeable differences in pressure distributions over the body. This is also very important as it impacts the maximum force that can be applied to the wearer. Reductions in the size of the thigh brace resulted in higher pressure concentrations on the anterior of the thigh. The more conformal fabric in the WeatherMAX waist belt also resulted in a better force distribution across the side of the pelvis. Given these results, it appears that the optimal design of a suit would include a large distribution area (lower pressures and higher stiffness) as well as a more conformal fabric, so long as the fabric's stretch does not significantly reduce the suit-human series stiffness.

Overall, this work was a preliminary investigation focusing on how design changes in the structured functional textile of exosuits affect suit stiffness and pressure distributions on the body. The testing methodology permits different contributions to the suit-human series stiffness to be identified, and shows potential for future investigations.

Additional work is required to more precisely determine the design changes that result in differences in suit performance. Finally, testing on humans with varying body compositions would provide more insight into the predominant role of human tissue in the suit-human series stiffness and the potential need for different suit designs for varying body compositions.

ACKNOWLEDGMENTS

REFERENCES

[1] Malcolm, P., Derave, W., Galle, S., and De Clercq, D., 2013. "A simple exoskeleton that assists plantarflexion can reduce the metabolic cost of human walking". *PloS one.* vol. 8.
[2] Malcolm, P., Derave, W., Galle, S., and De Clercq, D., 2011. "A Plantarflexion Assisting Exoskeleton Optimally Reduces Metabolic Cost of Walking When Actuation onset Coincides with Push Off Phase," presented in *International Society of Biomechanics Conference.*
[3] Lenzi, T., Carrozza, M. C., & Agrawal, S. K., 2013. "Powered hip exoskeletons can reduce the user's hip and ankle muscle activations during walking. *Neural Systems and Rehabilitation Engineering, IEEE Transactions on*, *21*(6), pp. 938-948.

[4] Kawamura, T., Takanaka, K., Nakamura, T., and Osumi, H., 2013. "Development of an orthosis for walking assistance using pneumatic artificial muscle," presented in *IEEE International Conference on Rehabilitation Robotics*.

[5] Oliver, J., Bouri, M., Ortlieb, A., Bleuler, H., and Clavel, R., 2013. "Development of an Assistive Motorized Hip Orthosis," presented in *IEEE International Conference on Rehabilitation Robotics*.

[6] Shimada, H., Hirata, T., Kimura, Y., Naka, T., Kikuchi, K., Oda, K., Ishii, K., Ishiwata, K, and Suzuki, T., 2009. "Effects of a robotic walking exercise on walking performance in community-dwelling elderly adults." *Geriatrics & gerontology international,* vol. 9, pp.372-381.

[7] Farris, R. J., Quintero, H. A., and Goldfarb, M., 2011. "Preliminary Evaluation of a Powered Lower Limb Orthosis to Aid Walking in Paraplegic Individuals," *IEEE Transactions on Neural Systems and Rehabilitation Engineering,* vol. 19.

[8] Neuhaus, P. D., Noorden, J. H., Craig, T. J., Torres, T., Kirschbaum, J., and Pratt, J. E., 2011. "Design and Evaluation of Mina: A Robotic Orthosis for Paraplegics," presented in *IEEE International Conference on Rehabilitation Robotics*.

[9] Kazerooni, H., and Steger, R., 2006. "The Berkeley Lower Extremity Exoskeleton," *Journal of Dynamic Systems, Measurement, and Control,* vol. 128, p. 14.

[10] Walsh, C. J., Endo, K., Herr, H. A., 2007. "Quasi-Passive Leg Exoskeleton for Load Carrying Augmentation," *International Journal of Humanoid Robotics, Special Issue: Active Exoskeletons*, vol. 4, pp. 487-506.

[11] Garcia, E., Sater, J. M., and Main, J., 2002. "Exoskeletons for human performance augmentation (EHPA): A program summary," *Journal-Robotics Society Of Japan,* vol. 20, pp. 44-48.

[12] Jezernik, S., Colombo, G., Keller, T., Frueh, H., and Morari, M., 2003. "Robotic orthosis Lokomat: a rehabilitation and research tool," *Neuromodulation: Technology at the Neural Interface,* vol. 6, pp. 108-115.

[13] Shen, B., Li, J., Bai, F., and Chew, C.M., 2013. "Development and Control of a Lower Extremity Assistive Device (LEAD) for Gait Rehabilitation," presented in *IEEE International Conference on Rehabilitation Robotics*.

[14] Hussain, S., Xie, S. Q., and Jamwal, P. K., 2012. "A Bio-Inspired Robotic Orthosis for Gait Rehabilitation," presented in *IEEE RAS/EMBS International Conference on Biomedical Robotics and Biomechatronics*.

[15] Winfree, K. N., Stegall, P., Agrawal, S. K., 2011. "Design of a Minimally Constraining, Passively Supported Gait Training Exoskeleton--Alex II," presented in *IEEE International Conference on Rehabilitation Robotics*.

[16] Shorter, K. A., Kogler, G. F., Loth, E., Durfee, W. K., and Hsiao-Wecksler, E. T., 2011. "A portable powered ankle-foot orthosis for rehabilitation," *Journal of Rehabilitation Research and Development,* vol. 48, pp. 459-72.

[17] Wehner, M., Quinlivan, B., Aubin, P. M., Martinez-Villalpando, E., Bauman, M., Stirling, L., Holt, K., Wood, R., and Walsh, C., 2013. "Design and Evaluation of a Lightweight Soft Exosuit for Gait Assistance," in *IEEE International Conference on Robotics and Automation*.

[18] Asbeck, A. T, Dyer, R., Larusson, A., and C. J. Walsh, "Biologically-inspired Soft Exosuit," presented at the International Conference on Rehabilitation Robotics, 2013.

[19] Asbeck, A. T., Schmidt, K., Walsh, C. J., 2014. "Soft Exosuit for Hip Assistance". *Robotics and Autonomous Systems*, In press.

[20] Ding, Y., Galiana, I., Asbeck, A., Quinlivan, B., De Rossi, S., and Walsh, C., 2014. "Multi-joint Actuation Platform for Lower Extremity Soft Exosuits". In the proceedings of the IEEE International Conference on Robotics and Automation (ICRA). Hong Kong, China. pp. 1327-1334.

[21] Asbeck, A., De Rossi, S., Holt, K., and Walsh, C., 2015 "A Biologically-Inspired Soft Exosuit for Walking Assistance." *International Journal of Robotics Research (IJRR)*, In press.

[22] Asbeck, A., De Rossi, S., Galiana, I., Ding, Y., and Walsh, C., 2015. "Stronger, Smarter, *Softer*: Next Generation Wearable Robots". *IEEE Robotics and Automation Magazine. 21(4)*, Dec, pp. 22-33.

[23] Asbeck, A., Schmidt, K., Galiana, I, Walsh, C., 2015. "Multi-joint Soft Exosuit for Gait Assistance". In the proceedings of the *International Conference on Robotics and Automation (ICRA)*. May.

[24] De Rossi, S., Bae, J., O'Donnell, K., Hendron, K., Holt, K., Ellis, T., Walsh, C., 2015. "Gait improvements in stroke patients with a soft exosuit." In the proceedings of the *Gait and Clinical Movement Analysis Society (GCMAS) Meeting*. Portland, OR; 2015.

[25] Park, Y. L., Chen, B. R., Young, D., Stirling, L., Wood, R. J., Goldfield, E., & Nagpal, R. (2011, September). Bio-inspired active soft orthotic device for ankle foot pathologies. In *Intelligent Robots and Systems (IROS), 2011 IEEE/RSJ International Conference on* (pp. 4488-4495). IEEE.

[26] Ding, Y., Galiana, I., Asbeck, A., De Rossi, S., Bae, J., Teles Santos, T.R., Lara Araujo, V., Lee, S., Holt, K.G., and Walsh, C., 2015. "Biomechanical and Physiological Evaluation of Multi-joint Assistance with Soft Exosuits". *Transactions on Neural Systems & Rehab*. In Review.

[27] Holloway, G., Daly, C., Kennedy, D., and Chimoskey, J., 1976. "Effects of external pressure loading on human skin blood flow measured by 133xe clearance". *J. Appl. Physiol.*, vol. 40, no. 4, pp. 597–600.

[28] Cool, J., 1989. "Biomechanics of orthoses for the subluxed shoulder". *Prosthet. Orthot. Int.*, vol. 13, no. 2, pp. 90–96.

[29] Pressure Sensitive Matricial Fabric. (n.d.). Retrieved April 18, 2015, from http://www.plugandwear.com/default.asp ?mod=product&cat_id=86,118&product_id=239

[30] Salerno, M., Mazzocchi, T., Ranzani, T., Mulana, F., Dario, P., & Menciassi, A. (2013, November). Safety systems in magnetically driven wireless capsule endoscopy. In *Intelligent Robots and Systems (IROS), 2013 IEEE/RSJ International Conference on* (pp. 3090-3095)..